

II METHODOLOGY

Navier-Stokes and full potential equations are the governing equations solved by the hybrid technique developed. This chapter explains the theory behind these equations and the technique used to numerically discretize them. The details for coupling of the two methods are also given. The formulation given below has been used in several fixed and rotary wing solvers that were developed by Sankar and his coworkers^{1, 2,3,4,5}.

2.1. Navier-Stokes Equations and Their Numerical Discretization

The Navier-Stokes equations are the most comprehensive relations that govern continuum flow for Newtonian fluids including air. These equations are composed of the conservation equations of mass, momentum and energy. There are only a few flow problems for which an analytical solution of Navier-Stokes equations is available where the flow geometry is very simple, usually two-dimensional, incompressible and where viscous effects may be neglected. Most fluid flow problems however do not fall into this category, and therefore require a numerical approximation of the governing equations.

The Reynolds averaged Navier-Stokes equations are used in this study for flow fields where all the turbulent fluctuating quantities are represented in a time averaged manner. In integral form for a deforming control volume, Ω , surrounded by surface, S , these equations may be written as

$$\frac{d}{dt} \iiint_{\Omega} q d\Omega + \iint_S (\vec{E}_I - q\vec{V}_{\Omega}) \cdot \vec{n} dS = \iint_S \vec{E}_V \cdot \vec{n} dS \quad (2.1)$$

Here \vec{V}_{Ω} is velocity associated with control volume deformation and q is the flow vector

$$q = \begin{Bmatrix} \rho \\ \rho u \\ \rho v \\ \rho w \\ e \end{Bmatrix} \quad (2.2)$$

with density, ρ , pressure, p , velocity components in the three principal directions, u , v , w , and energy per unit volume, e . \vec{E}_I and \vec{E}_V are the inviscid and viscous flux respectively. In physical coordinates they are written as in equation (2.3). The stress terms in Cartesian coordinates will be not explicitly given here because they are not used directly in the method and they can be found in any standard text. These terms will be presented later in the generalized coordinate system (computational space) that is used by the method.

$$\begin{aligned} \vec{E}_I &= E_{Ix}\vec{i} + E_{Iy}\vec{j} + E_{Iz}\vec{k} \\ \vec{E}_V &= E_{Vx}\vec{i} + E_{Vy}\vec{j} + E_{Vz}\vec{k} \end{aligned}$$

$$E_{Ix} = \begin{Bmatrix} \rho \\ \rho u^2 + p \\ \rho uv \\ \rho uw \\ u(e+p) \end{Bmatrix}, E_{Iy} = \begin{Bmatrix} \rho \\ \rho uv \\ \rho v^2 + p \\ \rho vw \\ v(e+p) \end{Bmatrix}, E_{Iz} = \begin{Bmatrix} \rho \\ \rho uv \\ \rho vw \\ \rho w^2 + p \\ w(e+p) \end{Bmatrix} \quad (2.3)$$

$$E_{Vx} = \begin{Bmatrix} 0 \\ \tau_{xx} \\ \tau_{yx} \\ \tau_{zx} \\ E_{x5} \end{Bmatrix}, E_{Vy} = \begin{Bmatrix} 0 \\ \tau_{xy} \\ \tau_{yy} \\ \tau_{zy} \\ E_{y5} \end{Bmatrix}, E_{Vz} = \begin{Bmatrix} 0 \\ \tau_{xz} \\ \tau_{yz} \\ \tau_{zz} \\ E_{z5} \end{Bmatrix}$$

A finite volume technique is used since deforming the computational grid is easier compared to finite difference schemes. In the finite volume method, integral formulations of the conservation laws are discretized directly in the physical space. On the other hand, in finite difference method, conservation laws are usually transformed from their Cartesian form onto a computational domain.

Applying the divergence theorem and the geometric conservation law⁶, equation (2.1) may be represented in semi-discrete form for a computational grid

$$\frac{d}{dt}(q\Omega_d) + \sum_{\text{faces}} (\tilde{\mathbf{E}}_I - q\vec{V}_{\text{Grid}}) \cdot \vec{n} \Delta S = \sum_{\text{faces}} \tilde{\mathbf{E}}_V \cdot \vec{n} \Delta S \quad (2.4)$$

This equation holds over a discrete control volume Ω_d , with cell faces of area ΔS and normal vector \vec{n} .

It has been shown that finite volume representation and finite difference formulation are equivalent⁴. Therefore finite difference formulation will be used for convenience as needed. For example, in the expression, $\delta_\xi E_i = \frac{E_{i+1/2} - E_{i-1/2}}{\Delta\xi}$, a central difference in finite volume form on the left side is equivalent to the finite difference representation on the right side. Keeping in mind this equivalence, the non-dimensional differential form of the governing equations in transformed coordinates is

$$q_\tau + F_\xi + G_\eta + H_\zeta = \frac{1}{\text{Re}} (R_\xi + S_\eta + T_\zeta) \quad (2.5)$$

The non-dimensionalization is performed using the free stream quantities for density, ρ_∞ ; velocity, a_∞ ; reference length, c ; and viscosity, μ_∞ . Reynolds number of the free stream is defined as $\text{Re} = \rho_\infty c a_\infty / \mu_\infty$.

Here q is the vector containing conserved flow variables, F , G and H are the transformed inviscid flux vectors and R , S and T are the transformed viscous stress vectors. The ξ , η , ζ and τ are the three coordinate directions and non-dimensional time in the generalized coordinate system. The flow vector q in equation (2.5) is defined as the physical flow vector over a cell volume, i.e.,

$$\mathbf{q} = \frac{1}{J} \begin{Bmatrix} \rho \\ \rho u \\ \rho v \\ \rho w \\ e \end{Bmatrix} = \Delta \text{Vol} \begin{Bmatrix} \rho \\ \rho u \\ \rho v \\ \rho w \\ e \end{Bmatrix} \quad (2.6)$$

Here first expression is in finite difference and the second expression is in finite volume form. J is the Jacobian of transformation given by

$$J = \frac{1}{y_{\xi}(x_{\zeta}z_{\eta} - x_{\eta}z_{\zeta}) + y_{\eta}(x_{\xi}z_{\zeta} - x_{\zeta}z_{\xi}) + y_{\zeta}(x_{\eta}z_{\xi} - x_{\xi}z_{\eta})} = \frac{1}{\Delta \text{Vol}} \quad (2.7)$$

and relates the physical and computational spaces. Velocity components u , v , and w are in x , y and z directions respectively. Energy per unit volume is

$$e = \frac{p}{\gamma - 1} + \frac{1}{2} \rho (u^2 + v^2 + w^2) \quad (2.8)$$

for calorically perfect gases. The contravariant velocities U , V , and W are the velocity components in the generalized coordinates, defined by

$$\begin{aligned} \frac{U}{J} &= \frac{\xi_t}{J} + \frac{\xi_x u}{J} + \frac{\xi_y v}{J} + \frac{\xi_z w}{J} = (\vec{V} - \vec{V}_{\text{Grid}}) \cdot \vec{n} \Delta S|_{i \pm 1/2} \\ \frac{V}{J} &= \frac{\eta_t}{J} + \frac{\eta_x u}{J} + \frac{\eta_y v}{J} + \frac{\eta_z w}{J} = (\vec{V} - \vec{V}_{\text{Grid}}) \cdot \vec{n} \Delta S|_{j \pm 1/2} \\ \frac{W}{J} &= \frac{\zeta_t}{J} + \frac{\zeta_x u}{J} + \frac{\zeta_y v}{J} + \frac{\zeta_z w}{J} = (\vec{V} - \vec{V}_{\text{Grid}}) \cdot \vec{n} \Delta S|_{k \pm 1/2} \end{aligned} \quad (2.9)$$

Here, ξ_{τ} , η_{τ} and ζ_{τ} are used to account for the grid velocity components (x_t, y_t, z_t) , and are simply, $-\vec{V}_{\text{Grid}} \cdot \vec{n} \Delta S$, in the finite volume scheme.

The inviscid (F, G, H), and viscous (R, S, T) flux vectors in the transformed coordinate directions are

$$F = \frac{1}{J} \begin{Bmatrix} \rho U \\ \rho u U + \xi_x p \\ \rho v U + \xi_y p \\ \rho w U + \xi_z p \\ (e + p)U - \xi_t p \end{Bmatrix}, \quad G = \frac{1}{J} \begin{Bmatrix} \rho V \\ \rho u V + \eta_x p \\ \rho v V + \eta_y p \\ \rho w V + \eta_z p \\ (e + p)V - \eta_t p \end{Bmatrix}, \quad H = \frac{1}{J} \begin{Bmatrix} \rho W \\ \rho u W + \zeta_x p \\ \rho v W + \zeta_y p \\ \rho w W + \zeta_z p \\ (e + p)W - \zeta_t p \end{Bmatrix}$$

$$R = \frac{1}{J} \begin{Bmatrix} 0 \\ \xi_x \tau_{xx} + \xi_y \tau_{xy} + \xi_z \tau_{xz} \\ \xi_x \tau_{xy} + \xi_y \tau_{yy} + \xi_z \tau_{yz} \\ \xi_x \tau_{xz} + \xi_y \tau_{yz} + \xi_z \tau_{zz} \\ \xi_x R_5 + \xi_y S_5 + \xi_z T_5 \end{Bmatrix}, \quad S = \frac{1}{J} \begin{Bmatrix} 0 \\ \eta_x \tau_{xx} + \eta_y \tau_{xy} + \eta_z \tau_{xz} \\ \eta_x \tau_{xy} + \eta_y \tau_{yy} + \eta_z \tau_{yz} \\ \eta_x \tau_{xz} + \eta_y \tau_{yz} + \eta_z \tau_{zz} \\ \eta_x R_5 + \eta_y S_5 + \eta_z T_5 \end{Bmatrix}$$

(2.10)

$$T = \frac{1}{J} \begin{Bmatrix} 0 \\ \zeta_x \tau_{xx} + \zeta_y \tau_{xy} + \zeta_z \tau_{xz} \\ \zeta_x \tau_{xy} + \zeta_y \tau_{yy} + \zeta_z \tau_{yz} \\ \zeta_x \tau_{xz} + \zeta_y \tau_{yz} + \zeta_z \tau_{zz} \\ \zeta_x R_5 + \zeta_y S_5 + \zeta_z T_5 \end{Bmatrix}$$

and they relate to their finite volume counter parts as

$$\begin{aligned} F &= \bar{E}_I \cdot \bar{n} \Delta S && \text{for faces } i+1/2, j, k \text{ and } i-1/2, j, k \\ R &= \bar{E}_V \cdot \bar{n} \Delta S \\ G &= \bar{E}_I \cdot \bar{n} \Delta S && \text{for faces } i, j+1/2, k \text{ and } i, j-1/2, k \\ S &= \bar{E}_V \cdot \bar{n} \Delta S \end{aligned} \tag{2.11}$$

$$\begin{aligned} H &= \bar{E}_I \cdot \bar{n} \Delta S && \text{for faces } i, j, k+1/2 \text{ and } i, j, k-1/2 \\ T &= \bar{E}_V \cdot \bar{n} \Delta S \end{aligned}$$

Viscous fluxes include shear stress terms

$$\begin{aligned}
\tau_{xx} &= \mu \left[\frac{4}{3} (u_\xi \xi_x + u_\eta \eta_x + u_\zeta \zeta_x) - \frac{2}{3} (v_\xi \xi_y + v_\eta \eta_y + v_\zeta \zeta_y + w_\xi \xi_z + w_\eta \eta_z + w_\zeta \zeta_z) \right] \\
\tau_{xy} &= \mu \left[(u_\xi \xi_y + u_\eta \eta_y + u_\zeta \zeta_y) + (v_\xi \xi_x + v_\eta \eta_x + v_\zeta \zeta_x) \right] \\
\tau_{xz} &= \mu \left[(u_\xi \xi_z + u_\eta \eta_z + u_\zeta \zeta_z) + (w_\xi \xi_x + w_\eta \eta_x + w_\zeta \zeta_x) \right] \\
\tau_{yy} &= \mu \left[\frac{4}{3} (v_\xi \xi_y + v_\eta \eta_y + v_\zeta \zeta_y) - \frac{2}{3} (u_\xi \xi_x + u_\eta \eta_x + u_\zeta \zeta_x + w_\xi \xi_z + w_\eta \eta_z + w_\zeta \zeta_z) \right] \\
\tau_{yz} &= \mu \left[(v_\xi \xi_z + v_\eta \eta_z + v_\zeta \zeta_z) + (w_\xi \xi_y + w_\eta \eta_y + w_\zeta \zeta_y) \right] \\
\tau_{zz} &= \mu \left[\frac{4}{3} (w_\xi \xi_z + w_\eta \eta_z + w_\zeta \zeta_z) - \frac{2}{3} (u_\xi \xi_x + u_\eta \eta_x + u_\zeta \zeta_x + v_\xi \xi_y + v_\eta \eta_y + v_\zeta \zeta_y) \right]
\end{aligned} \tag{2.12}$$

where Stokes hypothesis for bulk viscosity was used. The auxiliary functions are

$$\begin{aligned}
R_5 &= u \tau_{xx} + v \tau_{xy} + w \tau_{xz} + \frac{\mu}{\text{Pr}(\gamma - 1)} \left(\xi_x \frac{\partial a^2}{\partial \xi} + \eta_x \frac{\partial a^2}{\partial \eta} + \zeta_x \frac{\partial a^2}{\partial \zeta} \right) \\
S_5 &= u \tau_{xy} + v \tau_{yy} + w \tau_{yz} + \frac{\mu}{\text{Pr}(\gamma - 1)} \left(\xi_y \frac{\partial a^2}{\partial \xi} + \eta_y \frac{\partial a^2}{\partial \eta} + \zeta_y \frac{\partial a^2}{\partial \zeta} \right) \\
T_5 &= u \tau_{xz} + v \tau_{yz} + w \tau_{zz} + \frac{\mu}{\text{Pr}(\gamma - 1)} \left(\xi_z \frac{\partial a^2}{\partial \xi} + \eta_z \frac{\partial a^2}{\partial \eta} + \zeta_z \frac{\partial a^2}{\partial \zeta} \right)
\end{aligned} \tag{2.13}$$

In these relations ξ_x, η_z , etc. are metrics of the transformation, Pr is Prandtl number, a is the speed of sound and γ is the specific heat ratio. For turbulent flows, μ is replaced by $(\mu + \mu_T)$ where μ_T is the eddy viscosity defined by an appropriate turbulence model, and the Pr is replaced by $(\text{Pr} + \text{Pr}_T)$. Specific heat ratio is taken as 1.4, $\text{Pr} = 0.72$ and $\text{Pr}_T = 0.91$ in this study. Please note that such a formulation assumes air as a calorically perfect gas which is valid for helicopter rotor flows.

2.1.1. Treatment of Inviscid Fluxes

The semi discrete form of the governing equations (2.5) in generalized coordinates can be written as

$$\frac{dq}{dt} = \text{RHS} \quad (2.14)$$

where

$$\begin{aligned} \text{RHS} &= -(\delta_\xi F + \delta_\eta G + \delta_\zeta H) + \frac{1}{\text{Re}} (\delta_\xi R + \delta_\eta S + \delta_\zeta T) \\ &= \frac{-\sum_{i=1}^6 \bar{E}_I \cdot \Delta \bar{S}}{\text{Vol}} + \frac{\sum_{i=1}^6 \bar{E}_V \cdot \Delta \bar{S}}{\text{Vol}} \end{aligned} \quad (2.15)$$

Here the operators δ_ξ , δ_η and δ_ζ denote that the flux differences are computed in a finite volume manner. For example,

$$\delta_\xi F = \frac{F_{i+1/2,j,k} - F_{i-1/2,j,k}}{\Delta \xi} \quad (2.16)$$

and $\Delta \xi$ is taken to be unity. The first left hand side term in the above equation is the inviscid flux and the second term is viscous flux. The calculation of the inviscid fluxes is done by Roe's approximate Riemann solver⁷. Figure 2.1 shows a typical control volume surrounding the node (i,j,k) and to cell faces (i+1/2,j,k) and (i-1/2,j,k).

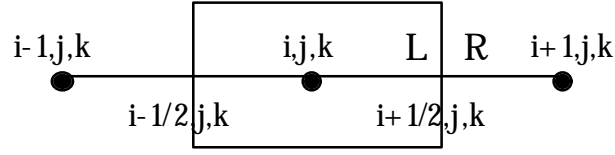


Figure 2.1: Cell Faces and the Control Volume

The inviscid fluxes are calculated as follows,

$$\bar{F}_{i+1/2,j,k} = 0.5 \left\{ (F_L + F_R) - |\bar{C}| (q_L - q_R) \right\} \quad (2.17)$$

The physical fluxes F , G and H in equation (2.17) are replaced by their numerical counterparts \bar{F} , \bar{G} , and \bar{H} which include the artificial dissipation contributions in the ξ , η and ζ directions respectively. The fluxes F_L and F_R are evaluated at the cell face $(i+1/2,j,k)$ using the information to the left and right of the cell interface. In equation (2.17), $C = \frac{\partial F}{\partial q}$, is the Jacobian matrix. The terms q_L and q_R are the flow vectors of primitive variables, $\{\rho, u, v, w, p\}^T$ evaluated to the left and right side of the cell interface $(i+1/2,j,k)$. The sketch below shows a typical control volume surrounding the node (i,j,k) and one of its six faces, $(i+1/2,j,k)$.

The physical fluxes F_L and F_R at the cell face $(i+1/2)$ are given by

$$F_L = \begin{Bmatrix} (\rho U)_i \\ (\rho U u)_i + (n_x)_{i+1/2} p_i \\ (\rho U v)_i + (n_y)_{i+1/2} p_i \\ (\rho U w)_i + (n_z)_{i+1/2} p_i \\ (\rho U h)_i + (n_t)_{i+1/2} p_i \end{Bmatrix} \quad F_R = \begin{Bmatrix} (r U)_{i+1} \\ (r U u)_{i+1} + (n_x)_{i+1/2} p_{i+1} \\ (r U v)_{i+1} + (n_y)_{i+1/2} p_{i+1} \\ (r U w)_{i+1} + (n_z)_{i+1/2} p_{i+1} \\ (r U h)_{i+1} + (n_t)_{i+1/2} p_{i+1} \end{Bmatrix} \quad (2.18)$$

The contravariant velocity U and the total enthalpy h per unit mass are defined by

$$\begin{aligned} \mathbf{U} &= u\mathbf{n}_x + v\mathbf{n}_y + w\mathbf{n}_z + n_t \\ \mathbf{h} &= (e + p)/\rho \end{aligned} \quad (2.19)$$

n_t is the grid speed of the cell face $(i+1/2)$ in the direction of the surface normal and is

$$n_t = -(x_\tau \bar{\mathbf{i}} + y_\tau \bar{\mathbf{j}} + z_\tau \bar{\mathbf{k}}) \cdot (n_x \bar{\mathbf{i}} + n_y \bar{\mathbf{j}} + n_z \bar{\mathbf{k}}) \quad (2.20)$$

The dissipation term is calculated as a sum of simple wave contributions depending on their wave speeds. To simplify the numerical computations, the matrix elements of $|\tilde{\mathbf{C}}|$ are multiplied analytically with the flow vector $q_R - q_L$. After some algebraic manipulations the resulting form is shown to be

$$|\tilde{\mathbf{C}}|(q_R - q_L) = |\tilde{\lambda}_1| \begin{Bmatrix} \Delta \rho \\ \Delta \rho u \\ \Delta \rho v \\ \Delta \rho w \\ \Delta e \end{Bmatrix} + \delta_1 \begin{Bmatrix} \tilde{\rho} \\ \tilde{\rho} \tilde{u} \\ \tilde{\rho} \tilde{v} \\ \tilde{\rho} \tilde{w} \\ \tilde{\rho} \tilde{h} \end{Bmatrix} + \delta_2 \begin{Bmatrix} 0 \\ n_x \\ n_y \\ n_z \\ \tilde{U}_c \end{Bmatrix} \quad (2.21)$$

where

$$\begin{aligned} \delta_1 &= C_1 \frac{\Delta \rho}{\tilde{\rho} \tilde{c}^2} + 0.5 C_2 \frac{\Delta U_c}{\tilde{c}} \\ \delta_2 &= C_1 \tilde{\rho} \Delta U_c - 0.5 C_2 \frac{\Delta p}{\tilde{c}} \\ C_1 &= -|\tilde{\lambda}_1| + 0.5(|\tilde{\lambda}_2| + |\tilde{\lambda}_3|) \\ C_2 &= |\tilde{\lambda}_2| - |\tilde{\lambda}_3| \end{aligned} \quad (2.22)$$

The characteristic wave speeds and the contravariant velocity \tilde{U}_c are defined by

$$\begin{aligned}\tilde{\lambda}_1 &= \tilde{U} ; \tilde{\lambda}_2 = \tilde{U} + \tilde{c} ; \tilde{\lambda}_3 = \tilde{U} - \tilde{c} \\ \tilde{U}_c &= (\tilde{u}\vec{i} + \tilde{v}\vec{j} + \tilde{w}\vec{k}) \cdot (n_x\vec{i} + n_y\vec{j} + n_z\vec{k})\end{aligned}\quad (2.23)$$

All the flow quantities with 'tilde' represent the Roe-averaged quantities which are defined for any given flow variable, ϕ other than ρ as:

$$\begin{aligned}\tilde{\rho} &= \sqrt{\rho_R \rho_L} \\ \tilde{\phi} &= \phi_L \left(\frac{1}{1 + \sqrt{\rho_R / \rho_L}} \right) + \phi_R \left(\frac{\sqrt{\rho_R / \rho_L}}{1 + \sqrt{\rho_R / \rho_L}} \right)\end{aligned}\quad (2.24)$$

2.1.1.1 Third Order MUSCL Scheme

The spatial order of the determined by the number of nodes from which information is utilized to calculate the primitive variables. For example, using $q_L = q_i$ and $q_R = q_{i+1}$ to the left and right sides leads to a first order scheme. The Monotone Upstream Centered Conservation Law (MUSCL) scheme⁸ is usually preferred:

$$\begin{aligned}q_L &= \{1 + [(1 - \kappa)\nabla + (1 + \kappa)\Delta] / 4\} q_i \\ q_R &= \{1 - [(1 + \kappa)\nabla + (1 - \kappa)\Delta] / 4\} q_{i+1}\end{aligned}\quad (2.25)$$

Here ∇ is the forward and Δ is the backward difference operator. Choosing a κ value of -1 gives a first order upwind scheme and a value of 1 gives a second order central difference scheme. A third order upwind scheme is obtained by giving κ a value of 1/3.

When the third order scheme is used, q_L at cell face $(i+1/2, j, k)$ requires information from nodes $i-1, i, i+1$, and similarly, q_R requires information from nodes $i, i+1, i+2$. Figure 2.2 shows the three point stencils for computing left and right primitive variables.

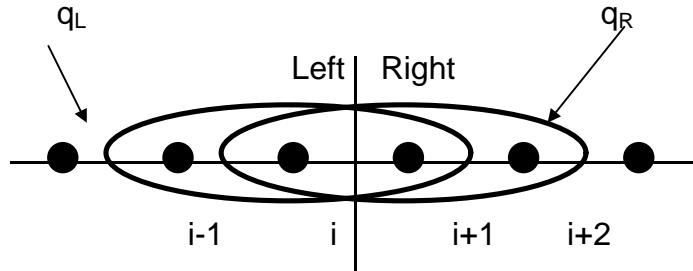


Figure 2.2 Three Point Stencil

2.1.1.2 Fifth Order Scheme

Higher order accuracy may be achieved by increasing the number of nodes where information is taken from. For example, if information from nodes $i-2$, $i-1$, i , $i+1$, $i+2$ are used to compute q_L at cell face $(i+1/2, j, k)$ and information from nodes $i-1$, i , $i+1$, $i+2$, $i+3$ are used to calculate q_R , then a fifth order scheme is obtained. Figure 2.3 shows a fixed five point stencil for calculation of q_L and q_R .

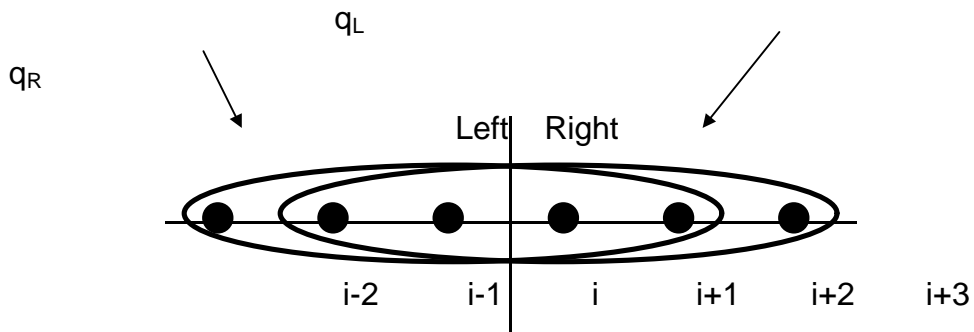


Figure 2.3 Fixed Five Point Stencil

In the hybrid solver, an option is available to use either third order or fifth order scheme for calculation of inviscid fluxes.

2.1.2. Treatment of Viscous Fluxes and Turbulence

The viscous flux terms in equation (2.15) are calculated at each time step and added to the inviscid flux contributions. The viscous terms in the three coordinate directions are calculated using formulas such as

$$\begin{aligned} \oint \bar{\mathbf{E}}_V \cdot \bar{\mathbf{n}} = & \bar{\mathbf{E}}_V \cdot \bar{\mathbf{n}} \Delta S \Big|_{i+1/2,j,k} + \bar{\mathbf{E}}_V \cdot \bar{\mathbf{n}} \Delta S \Big|_{i-1/2,j,k} + \bar{\mathbf{E}}_V \cdot \bar{\mathbf{n}} \Delta S \Big|_{i,j+1/2,k} + \\ & + \bar{\mathbf{E}}_V \cdot \bar{\mathbf{n}} \Delta S \Big|_{i,j-1/2,k} + \bar{\mathbf{E}}_V \cdot \bar{\mathbf{n}} \Delta S \Big|_{i,j,k+1/2} + \bar{\mathbf{E}}_V \cdot \bar{\mathbf{n}} \Delta S \Big|_{i,j,k-1/2} \end{aligned} \quad (2.26)$$

In the use of Reynolds averaged Navier-Stokes equations for flow field simulation, closure assumptions for modeling Reynolds stresses and turbulent transport of heat flux are needed. The eddy viscosity class of models, use the Boussinessq assumption which defines a scalar turbulent viscosity that connects the Reynolds stresses to the mean strain rate, and heat flux to the mean temperature gradient. The effective viscosity is obtained by adding the eddy viscosity to molecular viscosity. In the present study the classical algebraic Baldwin-Lomax turbulence model⁹ is used.

In this model the eddy viscosity, μ_T , is determined by splitting the flow field into an inner and outer layer and then using the appropriate one. Turbulent viscosity in the inner layer is defined as,

$$(\mu_T)_{\text{inner layer}} = \rho l_m^2 |\omega| \quad (2.27)$$

where $|\omega|$ is the mean vorticity, l_m is the mixing length.

$$|\omega| = \sqrt{\left(\frac{\partial w}{\partial y} - \frac{\partial v}{\partial z}\right)^2 + \left(\frac{\partial u}{\partial z} - \frac{\partial w}{\partial x}\right)^2 + \left(\frac{\partial v}{\partial x} - \frac{\partial u}{\partial y}\right)^2} \quad (2.28)$$

$$l_m = \kappa z D \quad (2.29)$$

Here $k = 0.4$ is the Von Karman constant, z is the normal distance from the wall, and D is Prantdl-Van driest damping factor defined as,

$$D = 1 - \exp\left(\frac{-z\rho_w\tau_w}{26\mu_w}\right) \quad (2.30)$$

In the outer layer turbulent viscosity is defined by

$$\begin{aligned} (\mu_T)_{\text{outer layer}} &= K_c C_{cp} \rho F_{\text{wake}} F_{\text{kleb}} \\ F_{\text{wake}} &= \min\left(z_{\text{max}} F_{\text{max}}, \frac{0.25z_{\text{max}} U_{\text{dif}}^2}{F_{\text{max}}}\right) \\ F(z) &= z|\omega| \left(1 - \exp\left(\frac{-z\rho_w\tau_w}{26\mu_w}\right)\right) \\ U_{\text{dif}} &= \left(\sqrt{u^2 + v^2 + w^2}\right)_{\text{max}} - \left(\sqrt{u^2 + v^2 + w^2}\right)_{\text{min}} \\ F_{\text{kleb}} &= \frac{1}{1 + 5.5 \left(\frac{0.3z}{z_{\text{max}}}\right)^6} \end{aligned} \quad (2.31)$$

where $K_c = 0.0168$ is Clauser's constant, and $C_{cp} = 1.6$ is an empirical constant. F_{kleb} is the Klebanoff intermittency factor. The switch between the two relations for eddy viscosity occurs at a distance measured from the solid surface where $(\mu_T)_{\text{inner layer}} = (\mu_T)_{\text{outer layer}}$.

2.1.3. Temporal Discretization and Diagonal ADI Factorization

Temporal discretization involves numerical integration of the semi discrete ODE given in equation (2.14). The right side, RHS, is clearly the sum over six faces of a cell surrounding the node (i,j,k) . This sum RHS in equation (2.15) may be viewed in two parts inviscid fluxes lumped into RHSI, and viscous fluxes lumped into RHSV.

$$\text{RHS} = \text{RHSI} + \text{RHSV} \quad (2.32)$$

$$\begin{aligned} \text{RHSI} &= \bar{F}_{i+1/2} - \bar{F}_{i-1/2} + \bar{G}_{j+1/2} - \bar{G}_{j-1/2} + \bar{H}_{j+1/2} - \bar{H}_{j-1/2} \\ \text{RHSV} &= R_{i+1/2} - R_{i-1/2} + S_{j+1/2} - S_{j-1/2} + T_{k+1/2} - T_{k-1/2} \end{aligned}$$

Equation (2.12) may be easily integrated using a number of explicit time marching schemes such as the Runge-Kutta two- and four step schemes. The following first order semi-implicit scheme for temporal discretization was chosen in this study.

$$\frac{d}{dt}(qV) = \text{RHSI}^{n+1} + \text{RHSV}^n \quad (2.33)$$

The equation (2.26) is a system of nonlinear algebraic equations due to the appearance of the quantities unknown at the $n+1$ level in the coefficients. A local linearization of the implicit fluxes proposed by Beam and Warming¹⁰ is done about the time level n to obtain a linear system of algebraic equations which may be solved by matrix inversions. The fluxes F , G and H are linearized about the time level n as

$$\begin{aligned} \bar{F}^{n+1} &= \bar{F}^n + \left(\frac{\partial \bar{F}}{\partial q} \right)^n \Delta q^n + O(\Delta \tau^2) \\ \bar{F}^{n+1} &= \bar{F}^n + A^n \Delta q^n \\ \bar{G}^{n+1} &= \bar{G}^n + \left(\frac{\partial \bar{G}}{\partial q} \right)^n \Delta q^n + O(\Delta \tau^2) \\ \bar{G}^{n+1} &= \bar{G}^n + B^n \Delta q^n \\ \bar{H}^{n+1} &= \bar{H}^n + \left(\frac{\partial \bar{H}}{\partial q} \right)^n \Delta q^n + O(\Delta \tau^2) \\ \bar{H}^{n+1} &= \bar{H}^n + C^n \Delta q^n \end{aligned} \quad (2.34)$$

where q is just the volume weighted property, and A , B and C are the 5×5 flux Jacobian matrices.

After substituting equation (2.34) into Equation (2.33) and transferring all the known quantities at time level n to the right hand side gives the following form

$$\begin{aligned} & \left[\mathbf{I} + \Delta t(A_{i+1/2}E_{\xi}^{+} - A_{i-1/2}E_{\xi}^{-} + B_{j+1/2}E_{\eta}^{+} - B_{j-1/2}E_{\eta}^{-} + C_{k+1/2}E_{\zeta}^{+} - C_{k-1/2}E_{\zeta}^{-}) \right] \mathbf{q}^{n+1} \\ & = -\Delta t(\text{RHS}^n) \end{aligned} \quad (2.35)$$

Here $E_{\xi, \eta, \zeta}^{\pm}$ is a shift operator, for example

$$E_{\xi}^{\pm} \Delta q_{i,j,k} = \Delta q_{i \pm 1, j, k} \quad (2.36)$$

By dropping terms on the left side various semi-implicit schemes can be constructed. In the present work $B_{j+1/2}E_{\eta}^{+}$ was dropped making the method semi-implicit in spanwise direction. Equation (2.35) may be viewed as a matrix system

$$[\mathbf{M}] \{ \Delta \hat{\mathbf{q}} \} = \{ \text{RHS} \} \quad (2.37)$$

The coefficient matrix M is a block penta-diagonal matrix. Exact inversion of this matrix using Gaussian elimination is computationally very expensive. Therefore, approximate factorization is used to split the coefficient matrix into two tri-diagonal matrices as

$$\begin{aligned} & \left[\mathbf{I} + \Delta t(A_{i+1/2}E_{\xi}^{+} - A_{i-1/2}) + \Delta t(E_{\xi}^{-} C_{k+1/2} E_{\zeta}^{+} - C_{k-1/2} E_{\zeta}^{-}) \right] = \\ & = \left[\mathbf{I} + \Delta t(A_{i+1/2}E_{\xi}^{+} - A_{i-1/2}) \right] \left[\Delta t(E_{\xi}^{-} C_{k+1/2} E_{\zeta}^{+} - C_{k-1/2} E_{\zeta}^{-}) \right] + O(\Delta t^2) \end{aligned} \quad (2.38)$$

and Equation (2.38) may be solved by a two step process.

A diagonal ADI factorization scheme proposed by Pulliam and Chaussee¹¹ may be used to further approximate the block tri-diagonal matrices to scalar tri-diagonal matrices. This option was used in the present study. Computation time is reduced by 30% without sacrificing the formal spatial and temporal accuracy. Details about the diagonalization are given in^{3,4} and will not be repeated here for clarity.

The right hand-side contains numerical viscosity to prevent odd-even errors. The left hand-side also requires a similar treatment. Therefore the matrices are modified by adding an implicit damping.

2.2. Full Potential Equation and Numerical Discretization

The potential flow equation is a highly simplified form of the Navier-Stokes equations. The flow field is assumed to be inviscid and irrotational in these relations. The mass conservation equation may be written in differential conservation form as

$$\rho_t + (\rho u)_x + (\rho v)_y + (\rho w)_z = 0 \quad (2.39)$$

The velocity in the full potential zone is decomposed into three parts. The free stream velocity, the perturbation potential velocity, and the induced velocity due to embedded wake. Equation below shows these three components,

$$\begin{aligned} \vec{V} &= \vec{\nabla}\phi + \vec{V}_w \\ u &= \phi_x + u_w = u_\infty + \phi_x + u_w \\ v &= \phi_y + v_w = v_\infty + \phi_y + v_w \\ w &= \phi_z + w_w = w_\infty + \phi_z + w_w \end{aligned} \quad (2.40)$$

In the present formulation, the full potential is denoted by ϕ and the perturbation potential is denoted by φ . Here the terms u_w , v_w , w_w are the induced vortical velocity components associated with the embedded wake elements. This velocity field is superimposed on the potential flow field to account for the wake shed from the rotor blades. Details on calculation of this vortical velocity, \vec{V}_w , will be given in the next chapter. The solution procedure given in this section is originally developed by Sankar et al.¹² but was modified in this study for inclusion of the induced velocity components.

In addition to the differential equation (2.39), a relation is needed to express the density in terms of the velocity potential, ϕ and its derivatives (i.e., the velocity components). This additional relation is the isentropic gas law

$$\frac{\rho}{\rho_{\infty}} = \left(\frac{a^2}{a_{\infty}^2} \right)^{\frac{1}{\gamma-1}} \quad (2.41)$$

where a is the speed of sound, given by the energy equation:

$$\frac{a^2}{\gamma-1} + \phi_t + \frac{u^2 + v^2 + w^2}{2} = \frac{a_{\infty}^2}{\gamma-1} + \frac{V_{\infty}^2}{2} \quad (2.42)$$

Using equations (2.41) and (2.42), equation (2.39) may be written as a second order hyperbolic partial differential equation for ϕ :

$$\left(\frac{\rho}{a^2} \right) [\phi_{tt} + \phi_x \phi_{xt} + \phi_y \phi_{yt} + \phi_z \phi_{zt}] = (\rho \phi_x)_x + (\rho \phi_y)_y + (\rho \phi_z)_z \quad (2.43)$$

This equation is transformed from physical to computational space using the same transformation as the Navier-Stokes equations. While a finite volume form of this equation can be developed, it is best described in a finite difference form for the perturbation potential as

$$\frac{\rho}{a^2 J} [\phi_{\tau\tau} + U \phi_{\xi\tau} + V \phi_{\eta\tau} + W \phi_{\zeta\tau}] = \left(\frac{\rho U}{J} \right)_{\xi} + \left(\frac{\rho V}{J} \right)_{\eta} + \left(\frac{\rho W}{J} \right)_{\zeta} + Q \quad (2.44)$$

Here Q is a source term associated with the rate of grid deformation and details about it may be found in Prichard¹³. The term vanishes for rigid grids and may be neglected for mildly deformed grids. This assumption is valid for the purpose of this study.

The terms U , V and W are the contravariant components of velocity and J is the Jacobian of the transformation between Cartesian and transformed coordinates. Note that U/J , V/J , W/J have interpretations as $\vec{V} \cdot \vec{n} \Delta S$ in a finite volume setting.

The contravariant velocity components may be written in velocity potential terms as

$$\begin{aligned}
 U &= \xi_t + A_1 \phi_\xi + A_2 \phi_\eta + A_3 \phi_\zeta \\
 V &= \eta_t + A_2 \phi_\xi + A_4 \phi_\eta + A_5 \phi_\zeta \\
 W &= \zeta_t + A_3 \phi_\xi + A_5 \phi_\eta + A_6 \phi_\zeta
 \end{aligned} \tag{2.45}$$

where

$$\begin{aligned}
 \xi_t &= -x_\tau \xi_x - y_\tau \xi_y - z_\tau \xi_z \\
 \eta_t &= -x_\tau \eta_x - y_\tau \eta_y - z_\tau \eta_z \\
 \zeta_t &= -x_\tau \zeta_x - y_\tau \zeta_y - z_\tau \zeta_z
 \end{aligned} \tag{2.46}$$

and x_τ , y_τ , and z_τ are grid velocities in three directions, and where

$$\begin{aligned}
 A_1 &= \xi_x^2 + \xi_y^2 + \xi_z^2 \\
 A_2 &= \xi_x \eta_x + \xi_y \eta_y + \xi_z \eta_z \\
 A_3 &= \xi_x \zeta_x + \xi_y \zeta_y + \xi_z \zeta_z \\
 A_4 &= \eta_x^2 + \eta_y^2 + \eta_z^2 \\
 A_5 &= \eta_x \zeta_x + \eta_y \zeta_y + \eta_z \zeta_z \\
 A_6 &= \zeta_x^2 + \zeta_y^2 + \zeta_z^2
 \end{aligned} \tag{2.47}$$

At a given time level n , the disturbance velocity potential ϕ and its temporal derivative ϕ_τ are known, and consequently all velocity components, speed of sound and density are also known. Equation (2.44) is a partial differential equation for ϕ with nonlinear coefficients. To circumvent the nonlinearities, ρ , a^2 , J , U , V , and W appearing on the left side, and the density appearing on the right side of equation (2.44) are computed at the time level n . The remaining quantities at the new time level $n+1$ are kept.

The temporal derivatives on the left hand side of equation (2.44) are discretized using two-point backward finite-difference operators, while the mixed time-space terms appearing on the left hand side are discretized using two-point upwind differences. In this respect, the left hand side of equation (2.44) is expressed as follows:

$$\left(\frac{\rho}{a^2 J}\right)_{i,j,k}^n \left[\bar{\delta}_\tau \bar{\delta}_\tau \varphi + U^n \bar{\delta}_\xi \bar{\delta}_\tau \varphi + V^n \bar{\delta}_\eta \bar{\delta}_\tau \varphi + W^n \bar{\delta}_\zeta \bar{\delta}_\tau \varphi \right]_{j,k} \quad (2.48)$$

At a typical grid node (i, j, k) , the first term inside the square brackets of equation (2.48) is expressed as

$$\bar{\delta}_\tau \bar{\delta}_\tau \varphi^{n+1} = \frac{\varphi^{n+1} - 2\varphi^n + \varphi^{n-1}}{(\Delta\tau)^2} = \frac{\Delta\varphi^{n+1} - \Delta\varphi^n}{(\Delta\tau)^2} \quad (2.49)$$

In the previous expression, $\Delta\varphi$ represents the change in the solution in two consecutive time steps, i.e., $\Delta\varphi^{n+1} = \varphi^{n+1} - \varphi^n$. The mixed space-time derivatives appearing in equation (2.48) are discretized using upwind-differencing for the spatial derivative, and two-point backward-differencing for the temporal derivative. In evaluating the second, third and fourth terms, the following expressions are used:

$$\begin{aligned} U \bar{\delta}_\xi \bar{\delta}_\tau \varphi &\equiv \frac{U + |U|}{2\Delta\tau} \left[\frac{\Delta\varphi_{i,j,k}^{n+1} - \Delta\varphi_{i-1,j,k}^{n+1}}{\Delta\xi} \right] + \frac{U - |U|}{2\Delta\tau} \left[\frac{\Delta\varphi_{i+1,j,k}^{n+1} - \Delta\varphi_{i,j,k}^{n+1}}{\Delta\xi} \right] \\ V \bar{\delta}_\eta \bar{\delta}_\tau \varphi &\equiv \frac{V + |V|}{2\Delta\tau} \left[\frac{\Delta\varphi_{i,j,k}^{n+1} - \Delta\varphi_{i,j-1,k}^{n+1}}{\Delta\eta} \right] + \frac{V - |V|}{2\Delta\tau} \left[\frac{\Delta\varphi_{i,j+1,k}^{n+1} - \Delta\varphi_{i,j,k}^{n+1}}{\Delta\eta} \right] \\ W \bar{\delta}_\zeta \bar{\delta}_\tau \varphi &\equiv \frac{W + |W|}{2\Delta\tau} \left[\frac{\Delta\varphi_{i,j,k}^{n+1} - \Delta\varphi_{i,j,k-1}^{n+1}}{\Delta\zeta} \right] + \frac{W - |W|}{2\Delta\tau} \left[\frac{\Delta\varphi_{i,j,k+1}^{n+1} - \Delta\varphi_{i,j,k}^{n+1}}{\Delta\zeta} \right] \end{aligned} \quad (2.50)$$

The flux-like terms appearing on the right hand side of Equation (2.44) are evaluated using two-point central-difference formulas, i.e.,

$$\begin{aligned}
\left[\left(\frac{\rho U}{J} \right)_{i,j,k} \right]_{\xi} &= \left(\frac{\rho U}{J} \right)_{i+\frac{1}{2},j,k} - \left(\frac{\rho U}{J} \right)_{i-\frac{1}{2},j,k} + O(\Delta \xi^2) \\
\left[\left(\frac{\rho V}{J} \right)_{i,j,k} \right]_{\eta} &= \left(\frac{\rho V}{J} \right)_{i,j+\frac{1}{2},k} - \left(\frac{\rho V}{J} \right)_{i,j-\frac{1}{2},k} + O(\Delta \eta^2) \\
\left[\left(\frac{\rho W}{J} \right)_{i,j,k} \right]_{\zeta} &= \left(\frac{\rho W}{J} \right)_{i,j,k+\frac{1}{2}} - \left(\frac{\rho W}{J} \right)_{i,j,k-\frac{1}{2}} + O(\Delta \zeta^2)
\end{aligned} \tag{2.51}$$

The density ρ in equation (2.51) is computed at the time level n , while the contravariant components of velocity are computed using mixed information from time level n and the new time level $n+1$ in order to reduce the number of diagonals in the final matrix of coefficients.

In order to maintain numerical stability in regions of supersonic flow, the numerical formulation must be constructed in such a way that it is consistent with the physical domain of dependence. For that purpose, the artificial compressibility method is used. Here, the density values that appear in $(\rho U/J)$ on the right side of equation (2.44) are biased in the direction of the flow if the flow is supersonic ($q > q^*$) using the procedure proposed by Shankar et al.¹⁴.

$$\tilde{\rho}_{i+1/2,j,k} = \rho_{i+1/2,j,k} - \frac{(\rho q)_{i+1/2,j,k} - (\rho^* q^*)_{i-1/2,j,k}}{q_{i,j,k}} \tag{2.52}$$

Here ρ^* and q^* represent sonic values of density and total velocity evaluated from

$$\begin{aligned}
q^* &= \sqrt{\left(\frac{1 + \frac{\gamma-1}{2} M_{\infty}^2}{\frac{\gamma+1}{2} M_{\infty}^2} \right)} U_{\infty} \\
\rho^* &= (q^* M_{\infty})^{2/(\gamma-1)}
\end{aligned} \tag{2.53}$$

When the above discretizations are employed, and using $\Delta\phi$, a system of linear equations are obtained as follows

$$\begin{aligned} & a_{i,j,k}^n \Delta\phi_{i,j,k-1}^{n+1} + b_{i,j,k}^n \Delta\phi_{i,j-1,k}^{n+1} + c_{i,j,k}^n \Delta\phi_{i-1,j,k}^{n+1} + d_{i,j,k}^n \Delta\phi_{i,j,k}^{n+1} \\ & + e_{i,j,k}^n \Delta\phi_{i+1,j,k}^{n+1} + f_{i,j,k}^n \Delta\phi_{i,j+1,k}^{n+1} + g_{i,j,k}^n \Delta\phi_{i,j,k+1}^{n+1} = R_{i,j,k}^n \end{aligned} \quad (2.54)$$

Here the coefficients $a_{i,j,k}^n, b_{i,j,k}^n, c_{i,j,k}^n, d_{i,j,k}^n, e_{i,j,k}^n, f_{i,j,k}^n, g_{i,j,k}^n$, and $R_{i,j,k}^n$ are functions of the transformation metrics, the contravariant velocities, the density ρ , the speed of sound a , and the time step Δt as shown below in equations (2.55) and (2.56),

$$\begin{aligned} a_{i,j,k} &= \left[\sigma_z \left(\frac{\rho W}{a^2 J \Delta \tau} \right)_{i,j,k}^n + \left(\frac{\rho A_6}{J} \right)_{i,j,k-1/2}^n \right] \\ b_{i,j,k} &= \left[\sigma_y \left(\frac{\rho V}{a^2 J \Delta \tau} \right)_{i,j,k}^n + \left(\frac{\rho A_4}{J} \right)_{i,j-1/2,k}^n \right] \\ c_{i,j,k} &= \left[\sigma_x \left(\frac{\rho U}{a^2 J \Delta \tau} \right)_{i,j,k}^n + \left(\frac{\rho A_1}{J} \right)_{i-1/2,j,k}^n \right] \\ d_{i,j,k} &= - \left[\left(\frac{\rho}{a^2 J \Delta \tau^2} \right)_{i,j,k}^n + \left| \left(\frac{\rho U}{a^2 J \Delta \tau} \right)_{i,j,k}^n \right| + \left| \left(\frac{\rho V}{a^2 J \Delta \tau} \right)_{i,j,k}^n \right| + \left| \left(\frac{\rho W}{a^2 J \Delta \tau} \right)_{i,j,k}^n \right| \right] \\ & - \left[\left(\frac{\rho A_1}{J} \right)_{i+1/2,j,k}^n + \left(\frac{\rho A_1}{J} \right)_{i-1/2,j,k}^n + \left(\frac{\rho A_4}{J} \right)_{i,j+1/2,k}^n + \left(\frac{\rho A_4}{J} \right)_{i,j-1/2,k}^n \right] \\ & - \left[\left(\frac{\rho A_6}{J} \right)_{i,j,k+1/2}^n + \left(\frac{\rho A_6}{J} \right)_{i,j,k-1/2}^n \right] \\ e_{i,j,k} &= \left[(\sigma_x - 1) \left(\frac{\rho U}{a^2 J \Delta \tau} \right)_{i,j,k}^n + \left(\frac{\rho A_1}{J} \right)_{i+1/2,j,k}^n \right] \\ f_{i,j,k} &= \left[(\sigma_y - 1) \left(\frac{\rho V}{a^2 J \Delta \tau} \right)_{i,j,k}^n + \left(\frac{\rho A_4}{J} \right)_{i,j+1/2,k}^n \right] \\ g_{i,j,k} &= \left[(\sigma_z - 1) \left(\frac{\rho W}{a^2 J \Delta \tau} \right)_{i,j,k}^n + \left(\frac{\rho A_6}{J} \right)_{i,j,k+1/2}^n \right] \end{aligned} \quad (2.55)$$

$$\begin{aligned}
R_{i,j,k} = & -\frac{1}{\Delta\tau^2} \left(\frac{\rho}{a^2 J} \right)_{i,j,k}^n \Delta\phi_{i,j,k}^n - \left(\frac{\rho U}{J} \right)_{i+1/2,j,k}^n + \left(\frac{\rho U}{J} \right)_{i-1/2,j,k}^n \\
& - \left(\frac{\rho V}{J} \right)_{i,j+1/2,k}^n + \left(\frac{\rho V}{J} \right)_{i,j-1/2,k}^n - \left(\frac{\rho W}{J} \right)_{i,j,k+1/2}^n + \left(\frac{\rho W}{J} \right)_{i,j,k-1/2}^n \quad (2.56)
\end{aligned}$$

where σ_x , σ_y , σ_z are switching terms arising from the upwind differencing used in the mixed derivative evaluations. For example, $\sigma_x = 0$ for $U < 0$ and $\sigma_x = 1$ for $U > 0$.

Application of equation (2.54) at the grid points result in a sparse pentadiagonal matrix system which may be expressed as:

$$[M] \{ \Delta\phi_{i,j,k} \}^{n+1} = \{ R_{i,j,k} \}^n \quad (2.57)$$

A three factor approximate factorization scheme is employed to solve the system of equations (2.57) efficiently.

$$[M_1][M_2][M_3] \{ \Delta\phi \}^{n+1} = \{ R \}^n \quad (2.58)$$

where the elements of matrices $[M_1]$, $[M_2]$, $[M_3]$ are recursively related to the coefficients of the matrix $[M]$ as given below,

$$\begin{bmatrix} d & e & f & g \\ c & d & e & f \\ b & c & d & e \\ a & b & c & d \end{bmatrix} = \begin{bmatrix} d & 0 & 0 & g \\ 0 & d & 0 & 0 \\ 0 & 0 & d & 0 \\ a & 0 & 0 & d \end{bmatrix} [d]^{-1} \begin{bmatrix} d & 0 & f & 0 \\ 0 & d & 0 & f \\ b & 0 & d & 0 \\ 0 & b & 0 & d \end{bmatrix} [d]^{-1} \begin{bmatrix} d & e & 0 & 0 \\ c & d & e & 0 \\ 0 & c & d & e \\ 0 & 0 & c & d \end{bmatrix} \quad (2.59)$$

This factorization results in errors of the form $\frac{g_{i,j,k} b_{i,j,k}}{d_{i,j,k}}$. All off-diagonal elements are of order Δt or higher. Thus the errors are of order Δt^2 or higher. Since $d_{i,j,k}$ includes contributions from all six nodes surrounding it, is more

diagonally dominant than that from classical ADI schemes. This scheme has been found to be very stable.

The solution to equation (2.58) is then obtained using a three-step procedure, where the three matrices on the left hand side are sequentially inverted. These matrices are tri-diagonal, and are efficiently inverted using the Thomas algorithm.

It should be noted that the above approximate factorization procedure is applicable to both quasi-steady as well as unsteady flow field solutions. In unsteady flow applications, the errors associated with the approximate factorization may be shown to be of order Δt^3 or higher.

2.3. Navier-Stokes/Full Potential Coupling

The boundaries that separate the two zones must be carefully handled to allow pressure waves and vorticity to propagate out to the far field without false reflections at the interface. A method had been developed and validated by Sankar and his coworkers for fixed wing¹⁵ and rotor⁵ flows modeled using a C-H grids. For the present integrated Navier-Stokes/Full Potential/Free Wake method a similar scheme is developed to pass flow information from zone to zone. However, owing to the different grid topology (H-H or H-O) and presence of the wake induced velocities, \vec{V}_w , a modified set of relations are developed for the flow quantities at the interfaces.

Figure 2.4 shows the computational domain and the boundaries that separate the two zones. For each block (upper and lower) there are three interfaces that surround the Navier-Stokes zone. The plane $k = k_{\text{match}}$ corresponds to the interface between the inner zone and the outer zone that lies in the normal direction. The planes $i = i_{\text{match}1}$ and $i = i_{\text{match}2}$ are the upstream and downstream interfaces in the chordwise direction, respectively. These three planes extend all the way in the spanwise direction. For convenience all the

formulation will be given only for the $k = k_{\text{match}}$ interface, since the same treatment is performed for the two remaining interfaces as well.

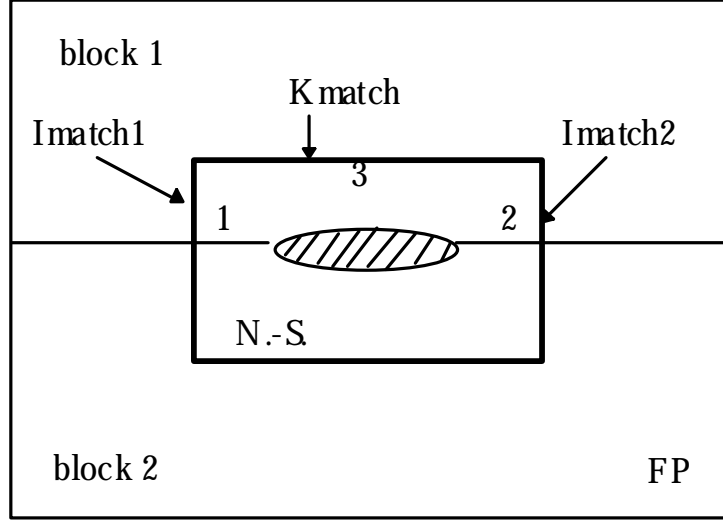


Figure 2.4: Partitioning of Computational Domain for H-O and H-H Topologies

2.3.1 Interface Conditions for the Inner Zone

The Navier-Stokes solver requires the flow properties (density, velocity, pressure) at the all interface planes. The velocity components are obtained by computing $\nabla\phi$ and adding wake induced velocities that carry effect of the far wake into the N.-S. zone,

$$\begin{aligned}
 u &= \phi_{\xi}\xi_x + \phi_{\eta}\eta_x + \phi_{\zeta}\zeta_x + u_w \\
 v &= \phi_{\xi}\xi_y + \phi_{\eta}\eta_y + \phi_{\zeta}\zeta_y + v_w \\
 w &= \phi_{\xi}\xi_z + \phi_{\eta}\eta_z + \phi_{\zeta}\zeta_z + w_w
 \end{aligned}
 \tag{2.60}$$

Then the energy equation is used to get temperature,

$$C_p T + \frac{u^2 + v^2 + w^2}{2} + \phi_t = C_p T_{\infty} + \frac{V_{\infty}^2}{2}
 \tag{2.61}$$

where C_p is the specific heat, and finally applying the isentropic law to get ρ and p .

$$\frac{T}{T_\infty} = \left(\frac{\rho}{\rho_\infty} \right)^{\gamma-1} \quad (2.62)$$

This formulation has been sufficient in the studies of Berezin⁵ and Sankar et al.¹⁵. However, the same interface boundary conditions showed an oscillatory behavior in convergence history when applied to an iced wing configuration¹⁶. Therefore Mello¹⁷ developed a set of non-reflecting interface conditions.

In these conditions, first the flow direction (inflow or outflow) and speed (subsonic or supersonic) are determined at the interface. For supersonic inflow all the flow information is taken from the outer zone, and for supersonic outflow all the information is extrapolated from the previous Navier-Stokes grid line. For subsonic flows, a combination of flow information from both zones are used based on Riemann invariants of the flow since an acoustic waves from the either side will effect the interface nodes. Figure 2.5 shows such acoustic waves traveling opposite directions.

These waves can be treated in a strictly time dependent manner, or in a quasi-steady manner. The latter is adequate if the purpose is of the boundary conditions is to eliminate false reflections at the interface. Further details and formulation is presented in Mello¹⁷ and will not be repeated here. However, in the next section some discussion about the waves crossing the interface is given. These improved set of interface boundary conditions are also available in the hybrid rotor solver as an option.

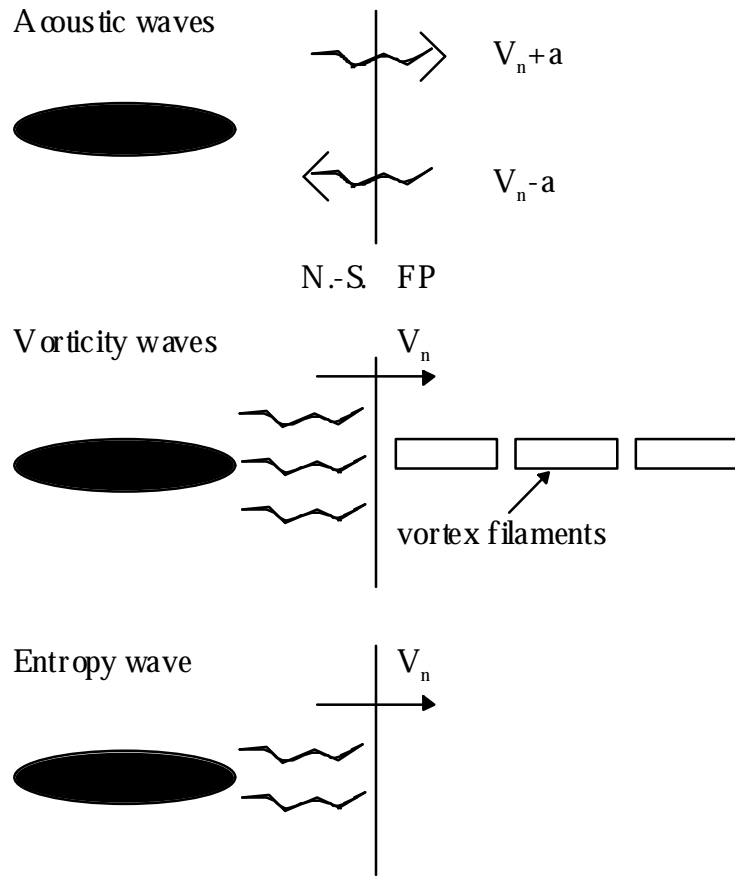


Figure 2.5 Treatment of Waves that Cross Zonal Interfaces

2.3.2 Interface Conditions for the Outer Zone

At a typical interface between the inner and outer zones, there are three types of waves that cross the boundary: acoustic, vorticity, and entropy waves. Since irrotational isentropic equations govern the outer zone all of this information can not be passed. Figure 2.5 shows the handling of the waves that cross the zonal interface. The acoustic waves are passed to the outer zone. The vortical waves are converted into lumped vortex elements or markers that are tracked in a Lagrangean fashion as discussed in the next chapter. The entropy wave carries entropy (i.e. changes in total pressure) at a velocity V_n .

This wave has to be ignored once it leaves the inner zone because the potential flow region is assumed isentropic.

The incoming acoustic wave to the outer zone is accounted for by matching the normal component of velocity at the interface plane between the potential flow and the viscous flow zones as,

$$V_n|_{NS} = V_n|_{FP} \quad (2.63)$$

If the $k = k_{\text{match}}$ interface is considered, this is equivalent to,

$$\frac{W}{J}|_{NS} = \frac{W}{J}|_{FP} \quad (2.64)$$

and by definition,

$$\frac{W}{J}|_{NS} = \frac{A_3\phi_\xi + A_5\phi_\eta + A_6\phi_\zeta}{J} \quad (2.65)$$

Solving for ϕ_ζ from equation (2.65) at the interface yields

$$\phi_\zeta = \frac{W|_{NS} - \phi_\xi A_3 - \phi_\eta A_5}{A_6} \quad (2.66)$$

Then ϕ_ζ at $k=k_{\text{match}}-1$ may be matched for the two zones using the difference formula:

$$\left(\phi_\zeta\right)_{i,j,k_{\text{match}}-1} \approx \frac{\phi_{i,j,k_{\text{match}}} - \phi_{i,j,k_{\text{match}}-2}}{2} \quad (2.67)$$

Equating (2.67) and (2.66) yields the interface condition for the full potential zone as

$$\Phi_{i,j,k_{\text{match}-2}} = \frac{-2(W|_{\text{NS}} - \phi_{\xi}A_3 - \phi_{\eta}A_5)}{A_6} + \Phi_{i,j,k_{\text{match}}} \quad (2.68)$$

Note that W contains the effect of induced velocity, since in the viscous zone the wake is self-generated. The effect of \bar{V}_w is taken out of W in equation (2.68) since the disturbance potential should not contain the wake-induced velocities. For the outer zone, this formulation combines information from the inner zone as well as the outer zone as seen in equation (2.68).